

STUDY ON SHUNT CURRENTS IN A MULTI-STACK VANADIUM FLOW BATTERY SYSTEM

Han-Wen Chou^a, Hwa-Jou Wei^a, Feng-Zhi Chang^b, Amornchai Arpornwichanop^c, Yong-Song Chen^{b*}

^aInstitute of Nuclear Energy Research, Atomic Energy Council, Taoyuan 32546, Taiwan

^bDepartment of Mechanical Engineering and Advanced Institute of Manufacturing with High-tech Innovations, National Chung Cheng University, Chiayi County 62102, Taiwan

^cComputational Process Engineering Research Unit, Department of Chemical Engineering, Faculty of Engineering, Chulalongkorn University, Bangkok 10330, Thailand

imeysc@ccu.edu.tw

Abstract: An all-vanadium redox flow battery (VRFB) is an energy storage device that uses the redox reaction of vanadium ions with different oxidation states. It has the advantages of quick conversion between charge and discharge processes, long operation life, separate power and energy capacity designs; as a result, it has been considered as one of potential candidates as energy storage systems for renewable energies. Because the electrolyte is electrically conductive, shunt currents occur within a multi-cell stack and within the piping system that connecting stacks. Shunt currents are affected by cell number in a single stack, stack number, dimensions of flow channels. In this study, a mathematical model is developed to determine shunt currents in a multi-stack system. The effect of stack number on charge transfer efficiency are predicted by this model. Results show that central stacks in a VRFB system provide more current. The maximum cell current decreases with increasing stack number.

Keywords: All-vanadium redox flow battery, multi-stack, shunt current, flow rate, charge transfer efficiency

Introduction

All-vanadium redox flow batteries (VRFBs) are devices that charge and discharge by the redox reaction of vanadium with different oxidation states. VRFBs have the advantages of long cycle life, low self-discharge, low maintenance cost, flexible design on stack power and environmental-friendly; as a result, they are considered as a potential energy storage system for renewable energy sources [1-3]. In a VRFB stack, multiple cells are connected in series for high voltage requirement. To meet the system voltage requirement, multiple VRFB stacks are connected in series in a system.

Because the electrolyte is electrically conductive, shunt currents occur in the manifolds and flow channels within the stacks and also in the piping system. The existence of shunt currents results in the decrease of electric capacity and energy conversation efficiency. As a result, it is important to understand the effect of shunt current on the battery performance and the effect of design parameters on shunt currents.

Xing et al. [4] developed a model to study shunt current in a VRFB stack based on the electrical circuit analog method. Their results suggested that increase of single cell power, reduction of cell number, and increase of the resistances of electrolytes in the manifolds and channels can help reduce shunt current loss. Tang et al. [5] investigated the effect of shunt current on efficiency and temperature variation within a 40-cell stack during standby condition by combining the shunt current model and thermal model. Their results showed that stack temperature was significantly increased due to the existence of shunt current within the VRFB stack.

It is challenging to measure shunt currents within a VRFB stack because it is not easy to install any current sensor in the manifolds and flow channels. Fink et al. [6] installed current sensors on the external hydraulic system of a 5-cell stack for the measurement of shunt currents. A mathematical model was also developed for the investigation of shunt current on coulombic efficiency. Results showed that inner cells within a stack discharge faster than outer cells. Yin et al. [7] developed a three-dimensional model to investigate the effect of shunt current distribution on coulombic efficiency. The model was validated by the experimental data and the results showed that short channel design caused a coulombic efficiency loss of approximately 23%.

Shunt currents could be reduced by increasing the electrical resistance of electrolyte in the flow path between cells;

as a result, longer and smaller cross-sectional area of flow path are preferred in designing a VRFB. However, the increase of flow resistance will cause the increase of pump consumption. The trade-off between shunt current loss and pump power consumption is a key issue on stack and system design. In this study, a mathematical model that can investigate the effect of flow path design on shunt current of a multi-stack system is developed. The distribution of shunt currents in the stack and in the piping system is predicted and the charge transfer efficiency is analyzed.

Modeling Methods

In order to simplify the model, the following assumptions were made.

1. Electrical potential is uniform throughout the active area.
2. Shunt currents in the inlet paths and outlet paths are the same in a single cell and in the piping system.
3. Temperature and electrolyte concentrations within the system are uniform.

The shunt currents within a VRFB stack and in the piping system were modeled as an equivalent electrical circuit, as shown in Figure 1. In the system, there are z VRFB stacks connected in series and each stacks consists of K cells, resulting in $M = Kz$ cells totally. The parameters $R_{pc,S}$, $R_{nc,S}$, $R_{pm,S}$, and $R_{nm,S}$ represent the equivalent resistances of electrolyte within the positive channel, negative channel, positive manifold, and negative manifold, respectively. The resistances of the electrolyte in the piping system are represented by $R_{pc,P}$, $R_{nc,P}$, $R_{pm,P}$, and $R_{nm,P}$.

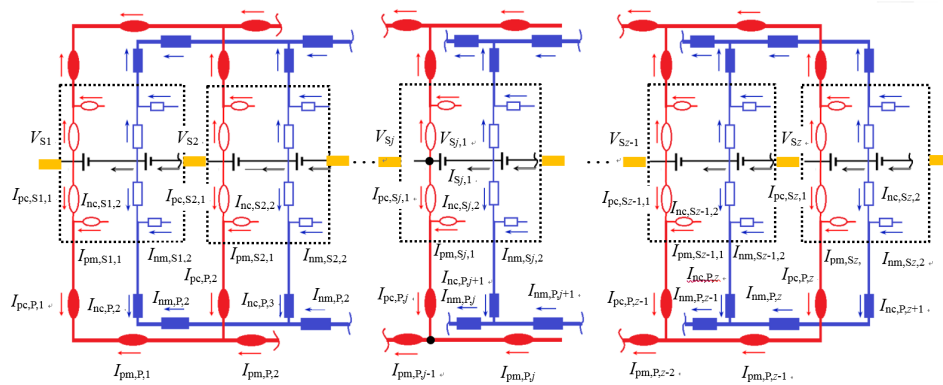


Figure 1. The equivalent electrical circuit of the system with multiple stacks in series.

Applying Kirchoff's law to the i -th cell of the equivalent electrical circuit for the stack results in linear equations.

$$I_{Sj,i} - I_{Sj,i-1} - 2I_{pc,Sj,i} - 2I_{nc,Sj,i} = 0 \tag{1}$$

$$I_{pc,Sj,i} + I_{pm,Sj,i} - I_{pm,Sj,i-1} = 0 \tag{2}$$

$$I_{nc,Sj,i} + I_{nm,Sj,i} - I_{nm,Sj,i-1} = 0 \tag{3}$$

$$V_{Sj,i} - R_{pc} I_{pc,Sj,i} + R_{pm} I_{pm,Sj,i} + R_{pc} I_{pc,Sj,i+1} = 0 \tag{4}$$

$$V_{Sj,i} - R_{nc} I_{nc,Sj,i} + R_{nm} I_{nm,Sj,i} + R_{nc} I_{nc,Sj,i+1} = 0 \tag{5}$$

where $I_{Sj,i}$ and $V_{Sj,i}$ represent the current and voltage of j -th stack in the system and i -cell in the stack.

In each stack, the positive electrolyte is connected with the positive channel of the positive piping system. The current and voltage relations can be modified as:

$$I_{Sj,1} - I_{Tj} - 2I_{pc,Sj,1} = 0 \tag{6}$$

$$I_{pc,Sj,1} + I_{pm,Sj,1} - I_{pc,Pj} = 0 \tag{7}$$

$$V_{Sj,1} - R_{pc} I_{pc,Sj,1} + R_{pm} I_{pm,Sj,1} + R_{pc} I_{pc,Sj,2} = 0 \tag{8}$$

where I_{Tj} is the overall current of a single stack. Similarly, the negative electrolyte is connected with negative piping system:

$$I_{nc,Sj,2} + I_{nm,Sj,2} - I_{nc,Pj} = 0 \tag{9}$$

The last single cell in each stack does not have a complete positive loop, the related equations are modified as:

$$I_{Sj,M} - I_{Sj,M-1} - 2I_{pc,Sj,M} - 2I_{nc,Sj,M} = 0 \tag{10}$$

$$I_{Sj,pc,M} - I_{Sj,pm,M-1} = 0 \tag{11}$$

$$I_{nc,M+1} - I_{nm,M} = 0 \tag{12}$$

In the piping system, similar equations for the current balance and voltage balance can be obtained by the same method:

$$I_{pc,P_j} + I_{pm,P_j} - I_{pm,P_{j-1}} = 0 \tag{13}$$

$$I_{nc,P_{j+1}} + I_{nm,P_{j+1}} - I_{nm,P_j} = 0 \tag{14}$$

$$V_{S_j} - R_{pc,S} I_{pc,S_{j,1}} - R_{pc,P} I_{pc,P_j} + R_{pm,P} I_{pm,P_j} + R_{pc,P} I_{pc,P_{j+1}} + R_{pc,S} I_{pc,S_{j+1,1}} = 0 \tag{15}$$

$$(V_{S_j} - V_{S_{j,1}}) - R_{nc,S} I_{nc,S_{j,2}} - R_{nc,P} I_{nc,P_{j+1}} + R_{nm,P} I_{nm,P_{j+1}} + R_{nc,P} I_{nc,P_{j+2}} + R_{nc,S} I_{nc,S_{j+2,2}} + V_{S_{j+1,1}} = 0 \tag{16}$$

The first and last stacks are special cases in this system:

$$I_{pc,P,1} + I_{pm,P,1} = 0 \tag{17}$$

$$I_{nc,P_{j+1}} + I_{nm,P_{j+1}} = 0 \tag{18}$$

$$I_{pc,P,z} + I_{pm,P,z-1} = 0 \tag{19}$$

$$I_{nc,P,z+1} - I_{nm,P,z} = 0 \tag{20}$$

The system voltage is the summation of stack voltage:

$$V_{SYS} = \sum_{j=1}^z V_{S_j} \tag{21}$$

The system current is the same with the stack current:

$$I_{SYS} = I_{T_j} \tag{22}$$

The cell voltage is assumed to be a function of operating current:

$$V_i = f(I_i) = V_{cell}^0 - R_c I_i \tag{23}$$

The resistance of the electrolyte can be determined by the dimension and geometry of the flow path. Shunt current and cell current are determined by this model. The overall unknown of the system is $5M-2$. The linear equations can be expressed in a matrix from:

$$\mathbf{V} = \mathbf{A}\mathbf{I} \tag{24}$$

where \mathbf{V} is the vector, consisting of cell voltages, \mathbf{A} is the matrix with resistances, and \mathbf{I} is the current vector to be solved. The solution process is similar to the previously published paper [8].

Results and Discussion

Voltage and current of each cell and shunt currents in the system are coupled together in this model. An iteration procedure was applied to solve this model. All cell currents were initially assumed to be the same; therefore, the initial cell voltages were the same. The cell voltages obtained from first and second calculations were very closed, as shown in Figure 2. In order to obtain accurate results, the results obtained by the second time calculation were used for analysis.

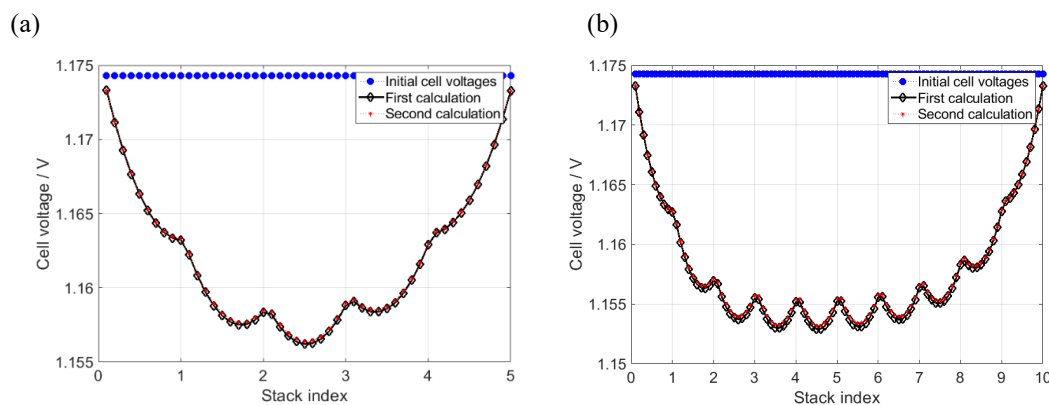


Figure 2. Convergence test of the model for (a) 5 20-cell stacks; and (b) 10 10-cell stacks.

There could be different configurations of cell number and stack number in a system. The following shows an example of designing an approximately 100-volt VRFB system with 100 cells. The stack number was designed as 5, 10, and 20 with cell numbers of 20, 10, and 5, respectively. The electrolyte conductivity and dimension of the flow channel and manifold in the stack can be obtained from our pervious study. The length of connected pipes varied with respect to stack size. Some distance was left between stacks for piping connection and maintenance, as shown in Fig. 3. The channel distance from the manifold of piping system to each stack is estimated as 15 cm.

Each cell thickness is estimated as 1 cm. The dimension of the piping system and corresponding electrolyte resistances are listed in Table 1.

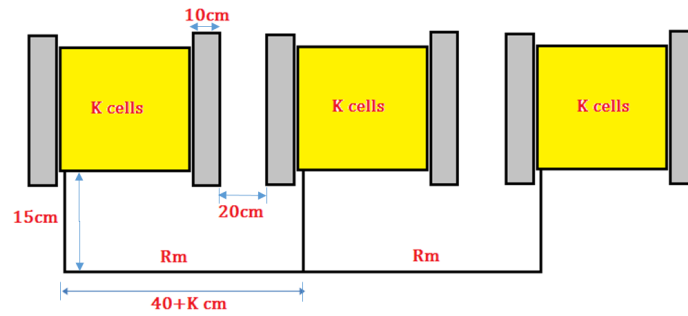


Figure 3. Dimension of piping system for electrolyte.

Table 1: Pipe length and resistance for various stack number.

Stack number, Z	Cell number in a stack, K	Pipe manifold length $L_m = 40 + K$ (cm)	Pipe manifold resistance R_{pm}, R_{nm} (Ω)
5	20	60	39.52
10	10	50	32.93
20	5	45	29.64

Figures 4(a), 4(b), and 4(c) present cell current distribution in each stack for 5, 10, and 20 stacks in series when the system is charged at 54 A. It can be seen that the cell currents are lower than 54 A. Part of charge was lost due to shunt current. For the 5-stack system, the lowest cell current in each stack is located at the central cells. However, for the 10-stack and 20-stack systems, the cell current of the first and last stack gradually decreases. It is due to the shunt current exiting in the flow channels of piping system. Figures 4(d), 4(e), and 4(f) present cell current distribution in each stack for 5, 10, and 20 stacks in series when the system is discharged at 54 A. The cell current distribution shows similar distribution as that in the charging process. Most central cells need to generate more current to compensate shunt current loss. It can also be observed that the cell current decreased with increasing stack number and the cell current distribution for most stacks became uniform. This is because the voltage difference between cells was reduced with decreasing cell number in a single stack.

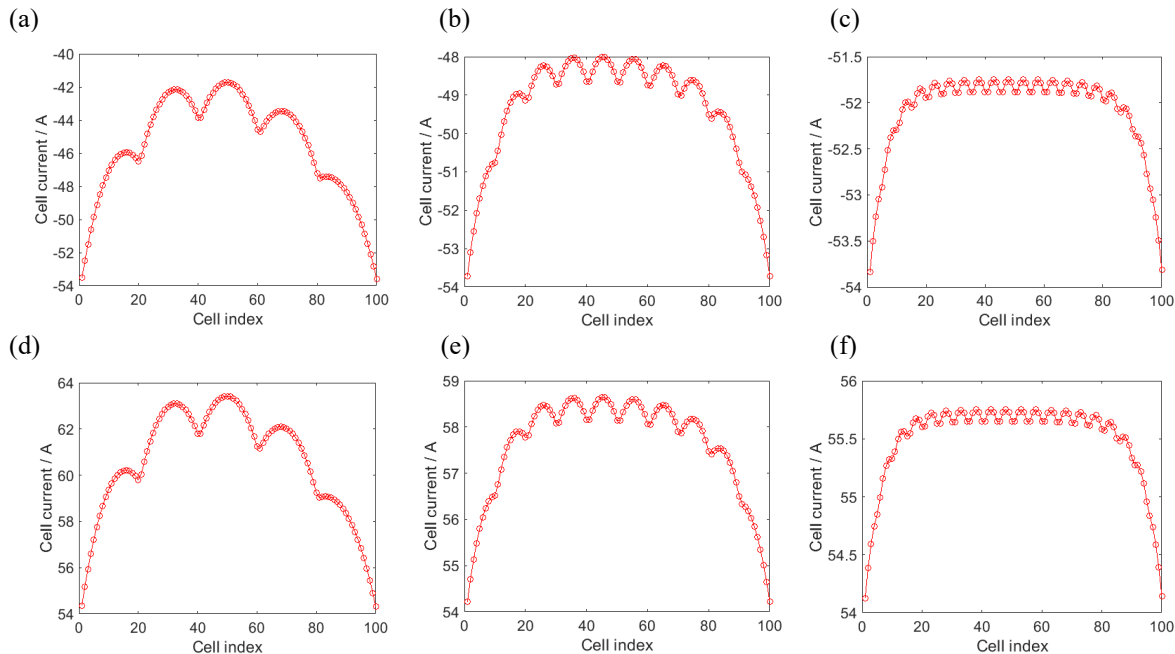


Figure 4. Cell current distribution during charge process for (a) 5 20-cell stacks; (b) 10 10-cell stacks; and (c) 20 5-cell stacks and during discharge process for (d) 5 20-cell stacks; (e) 10 10-cell stacks; and (f) 20 5-cell stacks.

Figures 5(a), 5(b), and 5(c) present shunt current in the flow channel and manifold of each stack for 5, 10, and 20 stacks in series when the system is charged at 54 A. In each stack, the maximum shunt current is located in the

manifolds due to the smallest electrolyte resistance. As the stack number increases, the shunt currents in the flow channel or manifold decrease. Due to the potential difference between cells and stacks. During the discharge process, the shunt current distribution shows similar trend.

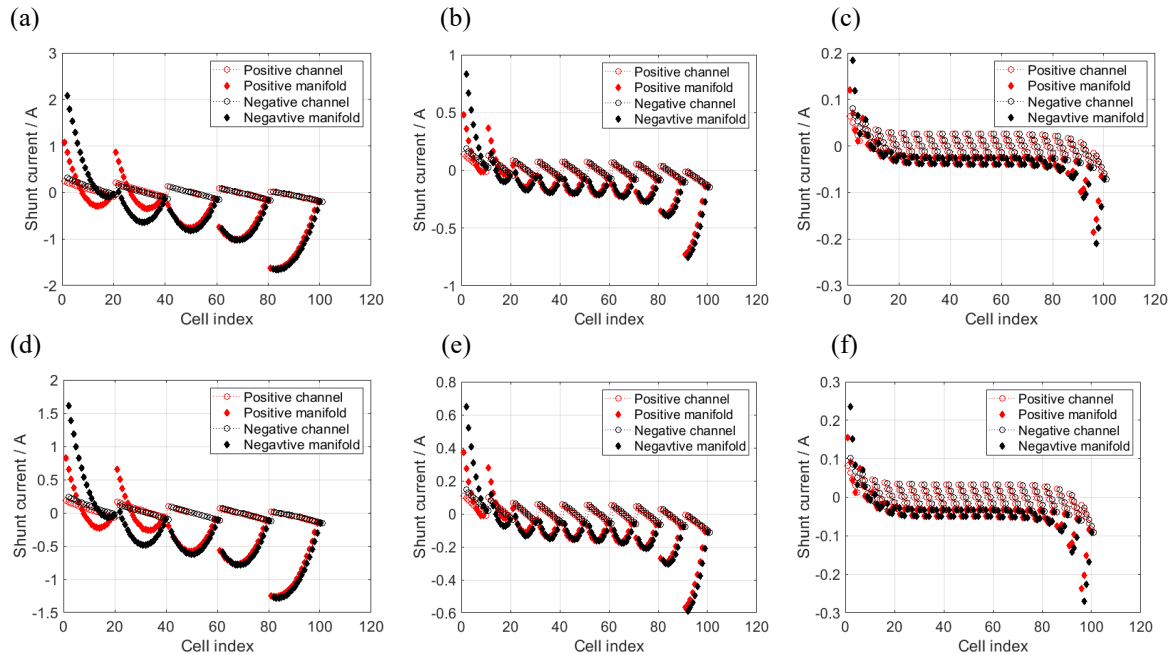


Figure 5. Shunt current distribution within the stacks during charge process for (a) 5 20-cell stacks; (b) 10 10-cell stacks; and (c) 20 5-cell stacks and during discharge process for (d) 5 20-cell stacks; (e) 10 10-cell stacks; and (f) 20 5-cell stacks.

Figures 6(a), 6(b), and 6(c) present shunt current in the flow channel and manifold of the piping system for 5, 10, and 20 stacks in series when the system is charged at 54 A. The maximum shunt current is located in the central manifold. In addition, the shunt currents in the first flow channel and last channel also showed relatively larger than those in the other flow channels. Because of the special location of first flow channels, shunt currents in the first stack converged to the first flow channel and first manifold. Similar Explanation can be applied for the discharge process, as shown in Figures 6(d), 6(e), and 6(f).

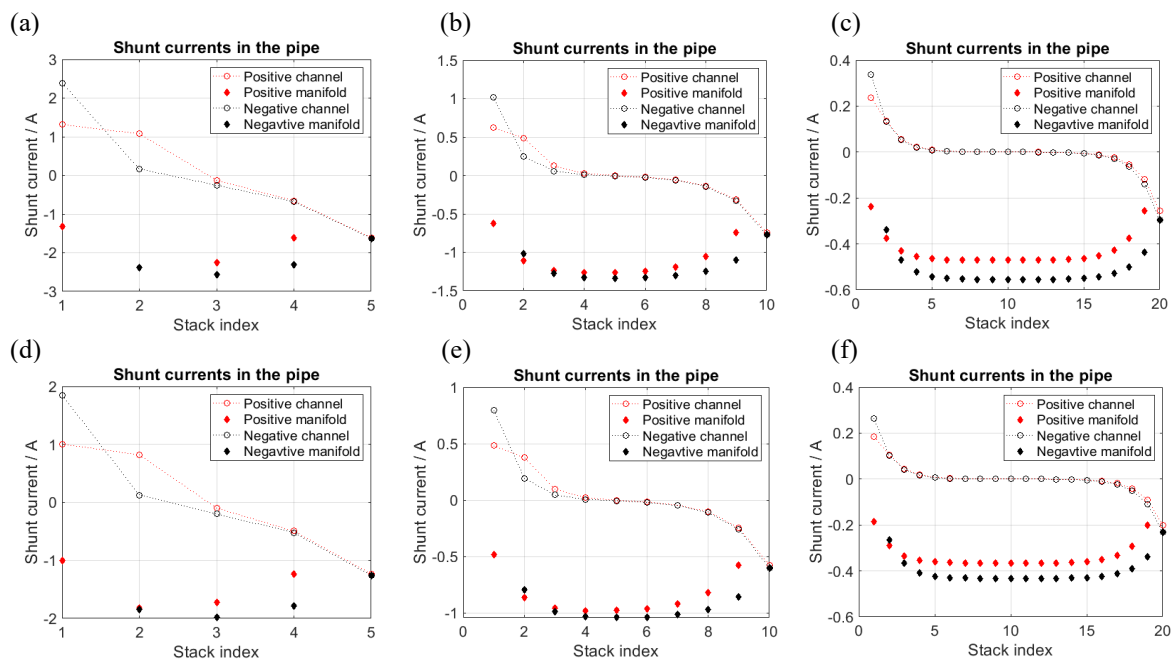


Figure 6. Shunt current distribution within the piping system during charge process for (a) 5 20-cell stacks; (b) 10 10-cell stacks; and (c) 20 5-cell stacks and during discharge process for (d) 5 20-cell stacks; (e) 10 10-cell

stacks; and (f) 20 5-cell stacks.

The charge efficiency is defined as the ratio of the power charged to each cell to the power applied to the system:

$$\varepsilon_{\text{charge}} = \frac{\sum(V_{\text{cell}} I_{\text{cell}})}{V_{\text{sys}} I_{\text{sys}}} \quad (25)$$

whereas the discharge efficiency is defined as the ratio of net power generated from the system to the power generated from each cell.

$$\varepsilon_{\text{discharge}} = \frac{V_{\text{sys}} I_{\text{sys}}}{\sum(V_{\text{cell}} I_{\text{cell}})} \quad (26)$$

The power difference between cells and system results from shunt current loss. The effect of stack number in a system with overall 100 cells on the efficiencies is shown in Table 2. As can be seen, the efficiencies increase with increasing stack number. As cell number in a single stack decreases, the maximum cell potential difference also reduces, resulting in lower shunt current. In addition, the electrolyte resistances in the piping system are usually larger than those within a stack, causing less shunt current. Although shunt current in a system can be reduced by increasing stack number, the pump power also increases due to increased pipes. A trade-off between pump power and shunt current need further investigation.

Table 2: Comparison of efficiencies of the system with various stack number.

Stack number	Charge efficiency	Discharge efficiency	Overall efficiency
5	0.896	0.926	0.830
10	0.943	0.957	0.902
20	0.975	0.968	0.944

Conclusion

Electrolyte of the VRFB is electrically conductive, causing shunt currents in the manifolds and flow channels within the stacks and also in the piping system. The existence of shunt currents results in power loss and performance drop. Shunt current is affected by cell number in a stack and stack number in a system. In this study, the effect of system configuration on shunt current is investigated by a mathematical model. The following conclusion can be drawn.

- (1) Shunt current shows quasi-symmetrically distribution within the connected stacks and the maximum shunt current is located in the central manifold of the piping systems.
- (2) Charge transfer efficiency increases with increasing stack number under a predetermined overall cell number in a system.

Acknowledgements

The authors would like to acknowledge the support from the Bureau of Energy (107-D0112), Ministry of Economic Affairs, Taiwan, ROC for this study.

References

- [1] C. Fabjan, J. Garche, B. Harrer, L. Jörissen, C. Kolbeck, F. Philippi, G. Tomazic, F. Wagner, The vanadium redox-battery: an efficient storage unit for photovoltaic systems, *Electrochim. Acta.* 47 (2001) 825–831.
- [2] M. Skyllas-Kazacos, G. Kazacos, G. Poon, H. Verseema, Recent advances with UNSW vanadium-based redox flow batteries, *Int. J. Energy Res.* 34 (2010) 182–189.
- [3] F. Díaz-González, A. Sumper, O. Gomis-Bellmunt, R. Villafafila-Robles, A review of energy storage technologies for wind power applications, *Renew. Sustain. Energy Rev.* 16 (2012) 2154–2171.
- [4] F. Xing, H. Zhang, X. Ma, Shunt current loss of the vanadium redox flow battery, *J. Power Sources.* 196 (2011) 10753–10757.
- [5] A. Tang, J. McCann, J. Bao, M. Skyllas-Kazacos, Investigation of the effect of shunt current on battery efficiency and stack temperature in vanadium redox flow battery, *J. Power Sources.* 242 (2013) 349–356.
- [6] H. Fink, M. Remy, Shunt currents in vanadium flow batteries: Measurement, modelling and implications for efficiency, *J. Power Sources.* 284 (2015) 547–553.
- [7] C. Yin, S. Guo, H. Fang, J. Liu, Y. Li, H. Tang, Numerical and experimental studies of stack shunt current for vanadium redox flow battery, *Appl. Energy.* 151 (2015) 237–248.
- [8] Y.S. Chen, S.Y. Ho, H.W. Chou, H.J. Wei, Modeling the effect of shunt current on the charge transfer efficiency of an all-vanadium redox flow battery, *J. Power Sources* 390 (2018) 168-175.